The small tunneling amplitude boson-Hubbard dimer

G. Kalosakas[1] and A. R. Bishop[2]

[1]Max Planck Institute for the Physics of Complex Systems, Germany
[2]Theoretical Division, Los Alamos National Laboratory, USA

Abstract

The boson-Hubbard dimer describes a BEC in a double well potential using the two mode approximation, which is relevant in the weak tunneling regime.
Analytical expressions for the energy eigenstates of this model are obtained by applying perturbation theory in the small tunneling amplitude limit. They are compared with the corresponding numerical solutions and the limits of their validity are determined.
These results are used for calculating the time evolution of the number difference of bosons between the two sites of the dimer. The analytical formulas concerning the time dependence of this observable for different initial conditions (completely localized states and coherent spin states) are compared with direct numerical solutions of the quantum system, as well as with the corresponding Gross-Pitaevskii (i.e. mean-field) dynamics.

The boson-Hubbard dimer Hamiltonian

A BEC in a double well potential with sufficiently distant local minima can be described by the two-mode approximation [1]

$$\mathcal{H} = -\kappa(b_1^\dagger b_2 + b_2^\dagger b_1) + U(b_1^\dagger b_1^\dagger b_1 b_1 + b_2^\dagger b_2^\dagger b_2 b_2)$$

$b_i^\dagger$, b_i: creation and annihilation operators of bosons at the i^{th} well.

κ: tunneling amplitude between the two wells.

U: interaction energy between pairs of atoms that are confined in a particular well.

$b_i = \int \phi_i^\star(\vec{r})\hat{\Psi}(\vec{r})d^3r, \quad i=1,2, \qquad \kappa = \frac{\Delta E}{2}, \qquad U = \frac{2\pi\hbar^2 a}{m_a}\int |\phi(\vec{r})|^4 d^3r$

Dimensionless quantities: U unit of energy, $k = \frac{\kappa}{U}$, $\tau = (U/\hbar)t$

Dimensionless Hamiltonian: $H = -k(b_1^\dagger b_2 + b_2^\dagger b_1) + (b_1^\dagger b_1^\dagger b_1 b_1 + b_2^\dagger b_2^\dagger b_2 b_2)$
The solutions depend on k and the total number of bobons $N = b_1^\dagger b_1 + b_2^\dagger b_2$.

Angular momentum representation:
$J_x = \frac{1}{2}(b_1^\dagger b_2 + b_2^\dagger b_1)$, $J_y = \frac{i}{2}(b_1^\dagger b_2 - b_2^\dagger b_1)$, $J_z = \frac{1}{2}(b_2^\dagger b_2 - b_1^\dagger b_1)$

$\Rightarrow \quad H = -2kJ_x + 2J_z^2$ (plus constant terms), $\quad J^2 = \frac{N}{2}\left(\frac{N}{2}+1\right)$, $\quad J_z = \frac{N_2-N_1}{2}$

Mean-field approximation

Mean-field approximation $\Rightarrow$ Discrete Nonlinear Schrödinger (DNLS) dimer [2]:

$$i\frac{dc_1}{d\tau} = -kc_2 + 2(N-1)|c_1|^2 c_1 \qquad i\frac{dc_2}{d\tau} = -kc_1 + 2(N-1)|c_2|^2 c_2$$

DNLS energy spectrum [3]: $E^{asym}_{extended} = \frac{N}{2} - Nk$, $E^{sym}_{extended} = \frac{N}{2} + Nk$,
$E_{localized} = \frac{N^2}{2} + \frac{k^2}{2}\frac{N}{N-1}$, for $k < k^{cr} = N-1$ (the localized solution bifurcates from the symmetric extended solution $E^{sym}_{extended}$, which becomes unstable below k^{cr}).

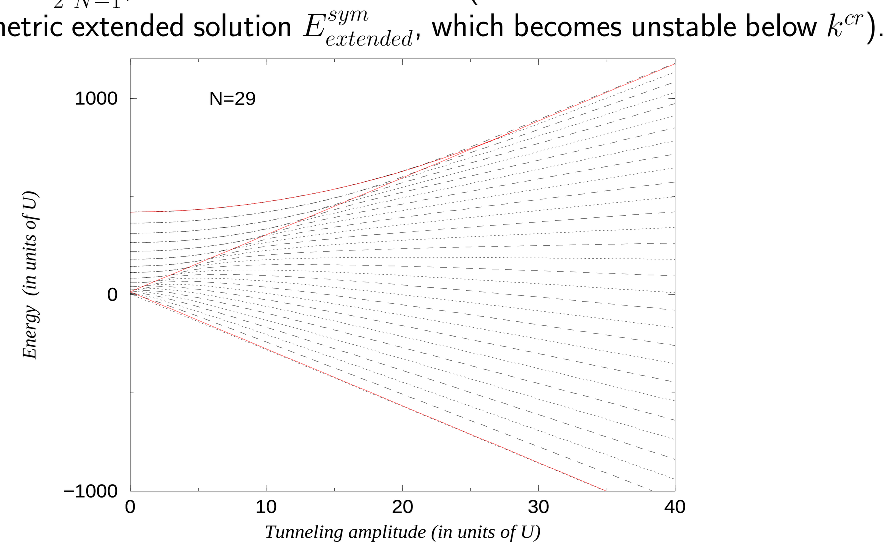

Fig.1: Energy spectrum of Hamiltonian H as a function of k, for $N=29$ bosons. Alternate dotted and dashed lines represent the $N+1$ quantum eigenvalues. These are degenerate by pairs in the small k limit. Continuous lines show the energies of the DNLS stationary states [4].

Energy eigenvalues for small k

For $k=0$ the $N+1$ eigenvalues form degenerate pairs of levels with energies

$$E^{(0)}_{m^\pm} = 2m^2, \qquad m = \tfrac{1}{2} \text{ or } 1, \ldots, \tfrac{N}{2}-1, \tfrac{N}{2}$$

m is positive integer (for even N) or half-integer (for odd N).
For even N the ground state $|0\rangle$ is non-degenerate with eigenvalue $E_{m=0} = 0$.
The corresponding eigenvectors are $|m^\pm\rangle = \frac{1}{\sqrt{2}}(|m\rangle \pm |-m\rangle)$,
where $|\pm m\rangle$ are the eigenvectors of J_z: $J_z|\pm m\rangle = \pm m|\pm m\rangle$.
The state $|m\rangle$ corresponds to the occupation of one site of the dimer by $\frac{N}{2}+m$ bosons and of the other site by the remaining $\frac{N}{2}-m$ bosons

As k increases from zero the degeneracy is gradually lifted, starting from the lower levels (the smaller m).
For fixed value of k the splitting $\Delta E_{m^\pm} = |E_{m^+} - E_{m^-}|$ decreases with m.
Up to second order in k the perturbative energy eigenvalues are given by [4]

$$E^{(2)}_{m^\pm} = 2m^2 + k^2\frac{J^2+m^2}{4m^2-1}, \quad \text{for } m \neq 1, \frac{1}{2}$$

$$E^{(2)}_{\frac{1}{2}^\pm} = \frac{1}{2} \mp k\sqrt{J^2+\frac{1}{4}} - \frac{k^2}{4}(J^2 - \frac{3}{4}), \quad \text{for odd } N$$

$$E^{(2)}_{1^\pm} = 2 + \frac{k^2}{6}(2J^2 \pm 3J^2 + 2), \quad \text{for even } N$$

The splittings $\Delta E_{m^\pm}$ of the levels $E_{m^\pm}$ for $m > 1$ (which are still degenerate up to second order) are of the order k^{2m} (see below). The higher energy levels form quasi-degenerate pairs for relatively small k

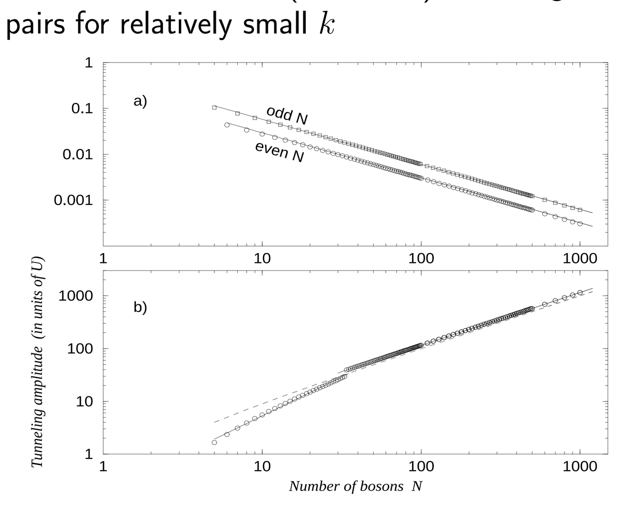

Fig.2: The value k_s at which the relative error of the perturbative energies, compared with the corresponding numerical ones, reaches 1%, as a function of the number N of bosons for **a)** the ground state and **b)** the most excited state. Circles and squares represent numerical results. Continuous lines represent fits with the formula $k_s = cN^a$. Ground state: $a \approx -1$ (for even or odd N). Most excited state: $a = 1$ for $N \geq 34$. The dashed line in b) plots $k = N-1$ [4].

Energy eigenvectors for small k

For $m \neq 0, 1, \frac{1}{2}$ the eigenvectors up to second order in k are [4]:

$$|h_{m^\pm}\rangle = A_m|m^\pm\rangle + B^+_m|(m+1)^\pm\rangle + B^-_m|(m-1)^\pm\rangle + C^+_m|(m+2)^\pm\rangle + C^-_m|(m-2)^\pm\rangle$$

where

$$A_m(k) = 1 - \frac{k^2}{4}\frac{4J^2m^2+J^2-4m^4+3m^2}{(4m^2-1)^2}, \qquad B^\pm_m(k) = \pm\frac{k}{2}\frac{\sqrt{J^2-m(m\pm1)}}{2m\pm1},$$
$$C^\pm_m(k) = \frac{k^2}{16}\frac{\sqrt{J^2-m(m\pm1)}\sqrt{J^2-(m\pm1)(m\pm2)}}{(m\pm1)(2m\pm1)}.$$

Regarding the experessions of $|h_0\rangle$, $|h_{1^\pm}\rangle$, and $|h_{\frac{1}{2}^\pm}\rangle$ see Ref. [4].

Evolution of the relative number difference

$$\langle J_z(\tau)\rangle = \sum_{n=m^\pm}\sum_{n'=m^\pm}\phi^\star_n\phi_{n'}\langle h_n|J_z|h_{n'}\rangle e^{i(E_n-E_{n'})\tau}$$

where ϕ_n are the projections of the initial condition: $\quad |\Psi(0)\rangle = \sum_{n=m^\pm}\phi_n|h_n\rangle$

Comparison with mean-field dynamics: $|c_2|^2 - |c_1|^2 \longrightarrow \frac{\langle J_z\rangle}{N/2} = \frac{N_2-N_1}{N}$

Completely localized initial state $|\Psi(0)\rangle = |\frac{N}{2}\rangle$

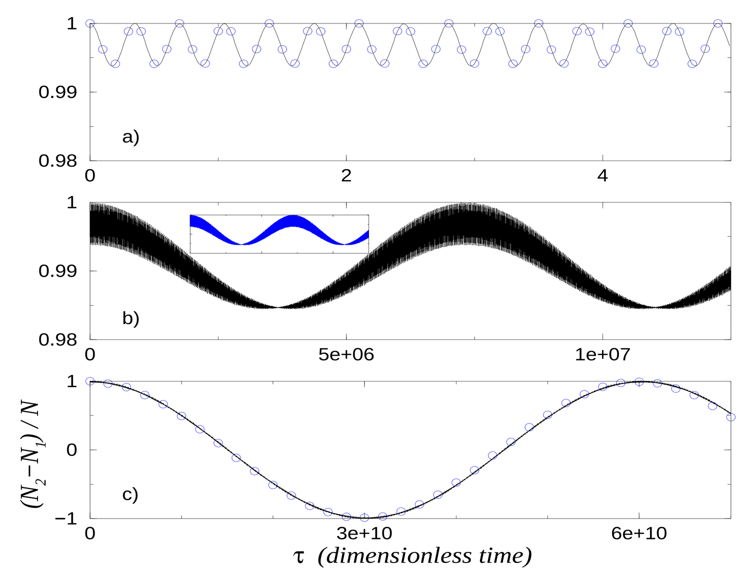

Fig.3: Evolution of the relative boson number difference between the two sites of the dimer at different time scales for $k=0.5$ in a system with $N=10$. Continuous lines represent numerical results. The inset in b) and the open circles in a) and c) correspond to analytical results [5].

$$\langle J_z^{(2)}(\tau)\rangle = \frac{N}{2}\cos(\omega_0\tau) + \frac{k^2 N}{4(N-1)^2}\times$$

$$\left[\frac{N}{2}[\cos(\omega_1\tau) - \cos(\omega_0\tau)] + 2\cos(\omega_\mu\tau)\cos(\frac{\omega_1}{2}\tau) - \cos(\omega_1\tau) - \cos(\omega_0\tau)\right]$$

where $\qquad \omega_\mu = 2(N-1) - k^2\frac{N+1}{N^2-4N+3}$

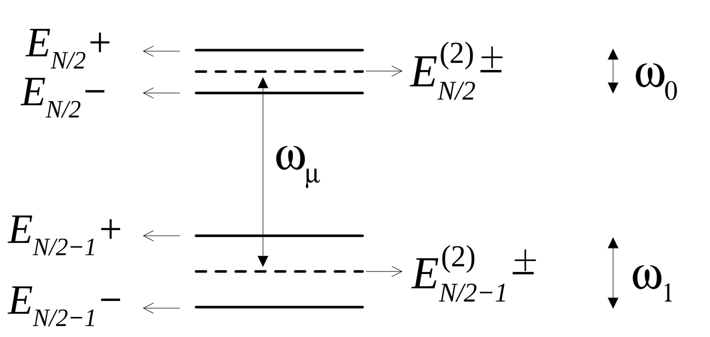

Fig.4: Schematic of the two upper quasi-degenerate pairs of energy levels. Up to second order in k they are still degenerate with energies $E^{(2)}_{\frac{N}{2}^\pm}$ and $E^{(2)}_{(\frac{N}{2}-1)^\pm}$, respectively. This energy difference provides the short time-scale oscillating frequency ω_μ. At higher order in k these quasi-degenerate pairs split, providing the frequencies ω_1 and ω_0 that characterize the collapses-revivals and the coherent tunneling between the two sites, respectively [6].

Following Ref. [7], the splitting of any quasi-degenerate pair is calculated as [5,8]:

$$\Delta E_{m^\pm} = k^{2m}\left[\tfrac{N}{2}(\tfrac{N}{2}+1) - m(m-1)\right]\frac{(\frac{N}{2}-m+2)\cdot\ldots\cdot(\frac{N}{2}+m-1)}{2^{2m-2}\,[\,(2m-1)!\,]^2}, \text{ for } m > 1$$

$$\Rightarrow \qquad \omega_0 = \Delta E_{\frac{N}{2}^\pm} = k^N\frac{N}{2^{N-2}\,(N-1)!}$$

$$\Rightarrow \qquad \omega_1 = \Delta E_{(\frac{N}{2}-1)^\pm} = k^{N-2}\frac{(N-1)(N-2)}{2^{N-4}\,(N-3)!}$$

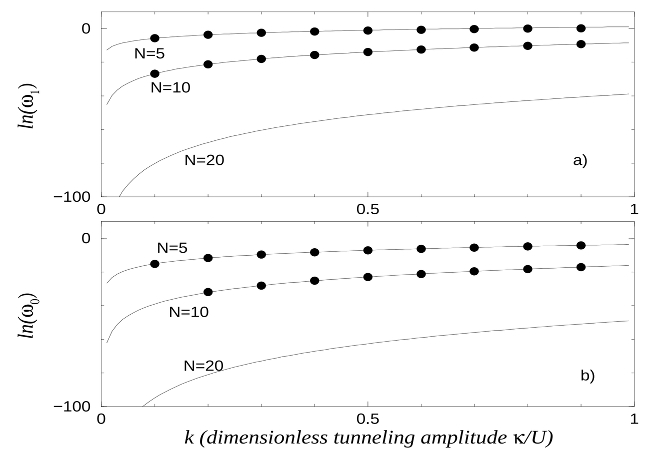

Fig.5: Logarithms of the characteristic frequencies **a)** ω_1, and **b)** ω_0, as a function of k for different numbers N of bosons. Continuous lines show analytical results, while filled circles correspond to numerical calculations [5].

Mean-field dynamics corresponds to the evolution shown in Fig.3a [9]:

$$\frac{N_2-N_1}{N} = dn\left((N-1)\tau\ ;\ \frac{2k}{N-1}\right) \longrightarrow 1 - \frac{2k^2}{(N-1)^2}\sin^2((N-1)\tau)$$

Coherent spin initial state

$$|\Psi(0)\rangle = \sin^{\frac{N}{2}}(\frac{\theta}{2})\cos^{\frac{N}{2}}(\frac{\theta}{2})e^{-i\frac{N}{2}\phi}\sum_{m=-\frac{N}{2}}^{m=\frac{n}{2}}\sqrt{\frac{N!}{(\frac{N}{2}+m)!\,(\frac{N}{2}-m)!}}\tan^m(\frac{\theta}{2})\,e^{-im\phi}|m\rangle$$

Zeroth-order terms ($\Rightarrow$ dominant frequency ω_e):
even N: $\qquad \langle J_z^0(\tau)\rangle =$

$$-\frac{N}{2}\cos(\theta) + \left(\frac{\sin(\theta)}{2}\right)^N P_1\cdot\left[\left(\tan^2(\tfrac{\theta}{2}) - \frac{1}{\tan^2(\frac{\theta}{2})}\right)(\cos(\omega_e\tau)-1) + 2\sin(2\phi)\sin(\omega_e\tau)\right]$$

where $\qquad \omega_e = E_{1^+} - E_{1^-} = k^2\frac{N}{2}\left(\frac{N}{2}+1\right), \qquad P_1 = \frac{N!}{(\frac{N}{2}+1)!(\frac{N}{2}-1)!}$

odd N: $\qquad \langle J_z^0(\tau)\rangle =$

$$-\frac{N}{2}\cos(\theta) + \frac{1}{2}\left(\frac{\sin(\theta)}{2}\right)^N P_{\frac{1}{2}}\cdot\left[\left(\tan(\tfrac{\theta}{2}) - \frac{1}{\tan(\frac{\theta}{2})}\right)(\cos(\omega_e\tau)-1) - 2\sin(\phi)\sin(\omega_e\tau)\right]$$

where $\qquad \omega_e = E_{1/2^-} - E_{1/2^+} = 2k\sqrt{\frac{N}{2}\left(\frac{N}{2}+1\right)+\frac{1}{4}}, \qquad P_{\frac{1}{2}} = \frac{N!}{(\frac{N}{2}+\frac{1}{2})!(\frac{N}{2}-\frac{1}{2})!}$

Coherent spin initial state (continued)

First-order terms: $\qquad \langle J_z^1(\tau)\rangle = \langle J_z^0(\tau)\rangle +$

$$k\left(\frac{\sin(\theta)}{2}\right)^N\left[C_1(\cos(\omega_e\tau)-1) + C_2\sin(\omega_e\tau) + \sum_{n=0 \text{ or } \frac{1}{2}}^{\frac{N}{2}-1} P_n\frac{N-2n}{2(2n+1)}A_n\right]$$

$$A_n = \tan^{2n+1}(\tfrac{\theta}{2})\,[\cos(F_n\tau+\phi) - \cos(\phi)] - \frac{1}{\tan^{2n+1}(\frac{\theta}{2})}\,[\cos(F_n\tau-\phi) - \cos(\phi)]$$

even N:

$$C_1 = P_1\cos(\phi)\left[\frac{N-2}{6}\left(\tan^3(\tfrac{\theta}{2}) - \frac{1}{\tan^3(\frac{\theta}{2})}\right) - \frac{N+2}{2}\left(\tan(\tfrac{\theta}{2}) - \frac{1}{\tan(\frac{\theta}{2})}\right)\right],$$
$$C_2 = P_1\left(\tan(\tfrac{\theta}{2}) + \frac{1}{\tan(\frac{\theta}{2})}\right)\left[\frac{N-2}{6}\sin(3\phi) - \frac{N+2}{2}\sin(\phi)\right],$$

$F_n = E_{n+1} - E_n = 4n+2, \quad n = 0, 1, \ldots, \frac{N}{2}-1 \quad \Rightarrow \quad F_n = 2, 6, 10, \ldots, 2N-2$

odd N:

$$C_1 = P_{\frac{1}{2}}\frac{N-1}{8}\cos(\phi)\left(\tan^2(\tfrac{\theta}{2}) - \frac{1}{\tan^2(\frac{\theta}{2})}\right),$$
$$C_2 = P_{\frac{1}{2}}\frac{N-1}{8}\sin(2\phi)\left(\tan(\tfrac{\theta}{2}) + \frac{1}{\tan(\frac{\theta}{2})}\right),$$

$F_n = E_{n+1} - E_n = 4n+2, \quad n = \frac{1}{2}, \frac{3}{2}, \ldots, \frac{N}{2}-1 \quad \Rightarrow \quad F_n = 4, 8, 12, \ldots, 2N-2$

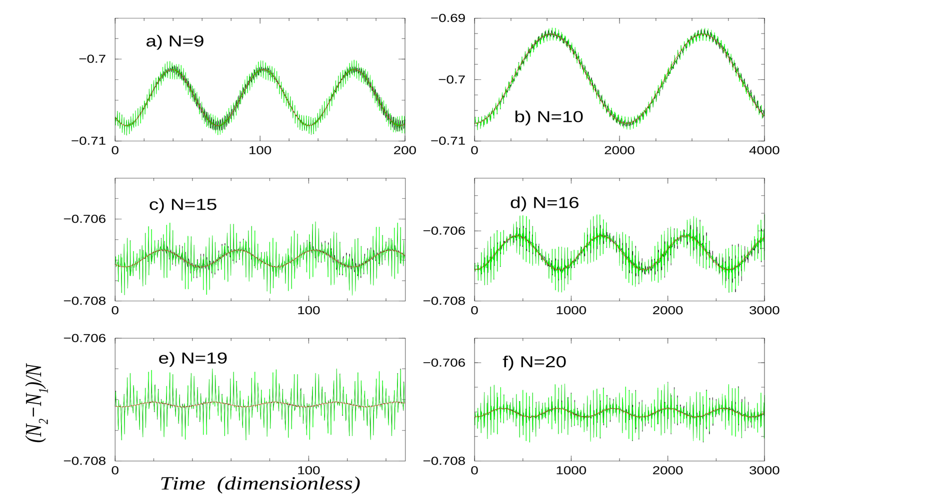

Fig.6: Evolution of the relative atom number difference, $\frac{2\langle J_z\rangle}{N}$, between the two sites of the double well for a coherent initial state with $\theta = \frac{\pi}{4}$ and $\phi = \frac{\pi}{2}$, in a system with $k = 0.01$, consisting of N =9, 10, 15, 16, 19, and 20 bosons, respectively. Black lines represent numerical results, red lines zeroth-order analytical results and green lines first-order analytical results [6].

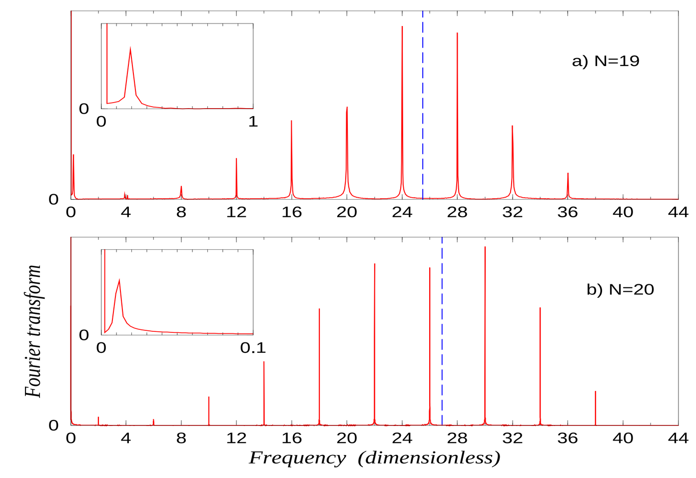

Fig.7: Fourier transform (red lines) of the numerical quantum evolution demonstrated in cases **a)** Fig.6e ($N=19$) and **b)** Fig.6f ($N=20$). Insets show a magnification of the spectra at the region of low frequencies, where ω_e appears. The unique frequency of the corresponding mean-field dynamics is also shown (dashed blue lines) [6].

Comparison with mean-field dynamics

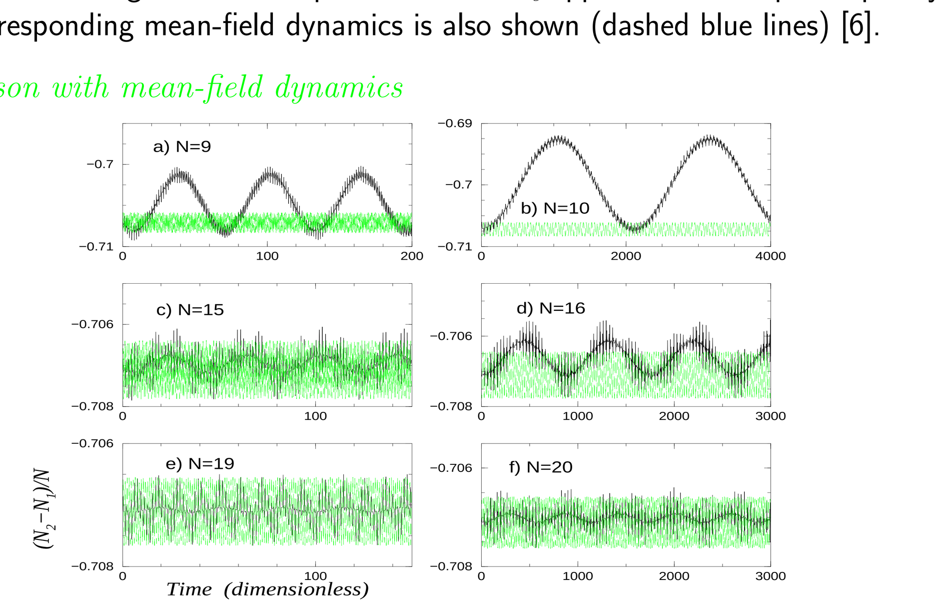

Fig.8: Evolution of the relative atom number difference, $|c_2|^2 - |c_1|^2$, in the mean-field approximation (green lines) for a coherent initial state with $\theta = \frac{\pi}{4}$ and $\phi = \frac{\pi}{2}$, in a system with $k = 0.01$, consisting of N =9, 10, 15, 16, 19, and 20 bosons, respectively. In all cases the dynamics is nearly harmonic. The numerically calculated quantum solution is shown for comparison (black lines) [6].

Conclusions

Perturbation theory in the small tunneling amplitude limit

- eigenvalues and eigenvectors up to second order
- splitting of the quasi-degenerate levels at higher order

Application in the evolution of a completely localized initial state

- small amplitude oscillations in short time-scales
- collapses and complete revivals in long time-scales
- coherent tunneling at even longer time-scales
- mean-field dynamics

Application in the evolution of a coherent initial state

- dominant frequency
- manifestation of the whole energy spectrum
- comparison with mean-field dynamics

References

[1] G.J. Milburn, J. Corney, E.M. Wright, and D.F. Walls, Phys. Rev. A **55**, 4318 (1997).

[2] E. Wright *et al.*, Physica D **69**, 18 (1993).

[3] J.C. Eilbeck, P.S. Lomdahl and A.C. Scott, Physica D **16**, 318 (1985).

[4] G. Kalosakas and A.R. Bishop, Phys. Rev. A **65**, 043616 (2002).

[5] G. Kalosakas, A.R. Bishop, and V.M. Kenkre, J. Phys. B **36**, 3233 (2003).

[6] G. Kalosakas, A.R. Bishop, and V.M. Kenkre, Phys. Rev. A **68**, 023602 (2003).

[7] L. Bernstein, J.C. Eilbeck, and A.C. Scott, Nonlinearity **3**, 293 (1990).

[8] S. Aubry, S. Flach, K. Kladko, and E. Olbrich, Phys. Rev. Lett. **76**, 1607 (1996).

[9] V.M. Kenkre and G.P. Tsironis, Phys. Rev. B **35**, 1473 (1987).